ORIGINAL ARTICLE

High Energy X-Ray Detection by MicroPattern Gaseous Detector

Saeedeh Khezripour [1], Mohammad Reza Rezaie Rayeni Nejad [2*]

[1] *Department of Molecular and Atomic Physics, Faculty of Modern Science and Technology, Graduate University of Advanced Technology, Kerman, Iran*

[2] *Department of Nuclear Engineering, Faculty of Modern Sciences and Technologies, Graduate University of Advanced Technology, Kerman, Iran*

*Corresponding Author: Mohammad Reza Rezaie Rayeni Nejad
Email: mr.rezaie.r@gmail.com

Received: 27 June 2024 / Accepted: 16 September 2024

Abstract

Purpose: The paper aims to discuss the response of the Micro-Mesh Gaseous Structure (Micromegas) detector to high-energy X-ray with 2.3 MeV energy using photon to neutron converters in addition to optimization of the detector components by Monte Carlo simulation.

Materials and Methods: Methods of using Micromegas are different in terms of energy and intensity of high-energy X-ray. Response of Micromegas detector to X-ray with 2.3 MeV by different photoneutron converters was calculated by Monte Carlo N Particle X-Version (MCNPX) code. The number of electrons in the drift and multiplication regions and the depth-dose in the various regions of the detector were measured to study the response of the Micromegas detector to high energy X-ray. Also, the thickness of the upper electrode, and the type of gas in the detector were studied and optimized.

Results: D_2O with 2×10^{-5} efficiency is the best target to convert photons with 2.3 MeV energy to neutrons. It is the proper convertor to change the high energy X-ray into a photoneutron that can be detected by Micromegas. The optimum thickness of the upper electrode is 0.0026 cm for air and P10 gas in the detector.

Conclusion: The results show that this detector can detect high-energy X-rays with energy above 2 MeV. The Monte Carlo results showed the output current of the Micromegas detector is 5.12 pA per one input hard X-ray photon.

Keywords: High Energy X-Ray; Gas Detector; Micromegas; D_2O; Photoneutron; Monte Carlo N Particle X-Version Code.

DOI:

1. Introduction

In general, high-energy X-ray detection is done by photographic film, scintillator, semiconductor detector, gas detector, etc. [1]. A gas detector is the simplest detector being sensitive to the effects of ionization of nuclear radiation. These types of detectors have a chamber containing certain volume of gas. Various types of gas detectors include ionization chambers, proportional chambers, and Geiger-Muller detectors [2]. Multi Wire Proportional Chamber (MWPC) sensitive to location has been primarily introduced by Charpak (1968) [3]. After that, in 1988, Anton Odd proposed a Micro Strip Gas Counter (MSGC) [4]. These detectors are characterized by their microstructure scale and their small multiplication region [5], which allows access to spatial resolution of a few micrometers, which is very useful in particle tracking or radiation imaging applications [6-12]. Today, these detectors have various designs, the general characteristic is having a small amplification region (less than 1 mm) between the cathode and the anode. One of these types of detectors is Micromegas detector that will be discussed in following.

In 1992, Micromegas detector was first designed and introduced by Charpak [13]. In 1996, this detector was introduced as an effective tool for the location-sensitive detection of high-flux particles. It found considerable popularity in high-energy particle physics applications [14]. The different regions of the charge production and the multiplication are important advantages of this type of detector. Hence, all electrons will have an equal multiplication factor. These detectors have been developed by different researchers to detect electron, proton, neutron, alpha, etc. [15-19]. In present research, high energy X-ray has been divided into two groups of higher and lower than 2 MeV, in terms of energy. Methods of using Micromegas are different in terms of energy and intensity of high energy X-ray. The Micromegas detectors have been investigated to detect photons in the energy range of less than 2 MeV [20, 21]. In the current research, the use of these detectors to detect X-rays with energy higher than 2 MeV is investigated using Monte Carlo simulation, and the dimensions of the detector are optimized using photon-to-neutron converter layers. Monte Carlo simulation using code MCNPX 2.7e (Monte Carlo N Particle Version 2.7e) is performed which can track 32 atomic and nuclear particles. When photoneutrons interact with the gas and components inside the detector, various processes occur such as neutron activation and creation of a compound nucleus. Compound atoms and nuclei cause ionization of the gas in the active area of the detector, and due to the presence of an electric field inside the detector, electron multiplication occurs and there is a possibility of creating the SQS phenomenon. Converter layers in Micromegas detectors have been used to detect neutrons [22], but there has been no report on the use of converter layers in these detectors to detect high-energy photons. In fact, the novelty of the work is the use of appropriate converter layers to detect high-energy photons by the Micromegas detector. The response of the detector depends on two factors: the type of converter and the energy of high-energy X-rays which will be analyzed in the following.

2. Materials and Methods

2.1. Design and Performance of the Detector

The Micromegas detector was designed according to Figure 1 to detect an X-ray radiation. The Micromegas detector works on the basis of the amplification of electric charges produced by the ionization of gas atoms by primary radiation. The neutrons that are produced in the converter as a result of high-energy X-ray photons reach the upper electrode and due to interaction with it, low-energy photons and electrons are produced and cross the driving region. The converter layer can be of different materials such as W, D_2O, etc. The gas-filled area between the cathode and anode parallel plates is divided into two parts by a mesh structure with fine holes named micromesh.

The rays received from the X-ray converter create ion pairs in the space between the cathode and the micromesh. The ionization electrons move towards micromesh through a relatively weak electric field which is lower than the necessary threshold for multiplication. The thickness of the ionization zone is usually several millimeters and it is large enough to produce a sufficient number of ion pairs for an ionizing particle with low penetration. In the absence

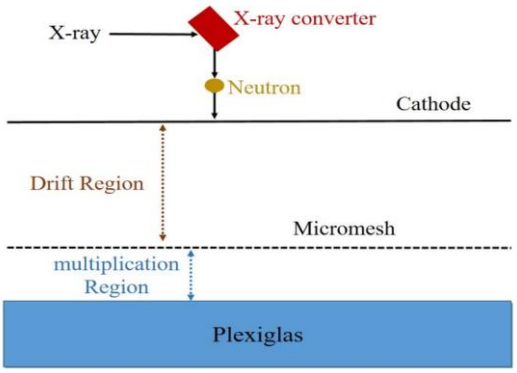

Figure1. Overview of the Micromegas detector irradiated by X-ray

of an electric field, the produced ion-electron pairs are recombined. By applying the electric field in the range of the proportional region, the electrons move towards the micromesh and the ions move towards the cathode. When the electrons reach near the micromesh, they are exposed to a strong electric field gradient in the propagation region, under the influence of this electric field, they accelerate and get the necessary energy to create the secondary electron-ion pairs, and then the phenomenon of electron avalanche occurs.

In fact, the Micromegas detectors include a small propagation area and produce signals of the order of 100 nanoseconds. The micromesh is made by various microfabrication techniques and its transparency is high for ionization electrons which means that many ionization electrons pass through the micromesh and continue moving towards the anode. But the electric field in the area between the micromesh and the anode causes a gain between 10^3 and 10^4, although this field is much higher than the value required to form an avalanche. The space between the micromesh and the anode plate is kept small (of the order of 100 micrometers) so that this required electric field can be reached by using appropriate voltages and also help in the formation of fast pulses. By choosing a suitable voltage, most of the positive ions produced in ion avalanches are collected by the micromesh. By minimizing the drift distance, these positive ions can improve the rapid recovery of space charge effects and provide the ability to work at high frequencies. This small gap is usually achieved by using insulating columns between the micromesh and the anode. Small and unavoidable dimensional changes in the gas thickness do not significantly affect ion avalanches, because smaller gas thicknesses can be neutralized by higher electric fields in that region. Because the produced avalanches are almost the same size, the amplitude of the pulse produced by the anode is proportional to the number of ion pairs formed in the ionization area of the chamber.

2.2. Monte Carlo Simulation

MCNPX code is one of the most powerful calculation codes based on the Monte Carlo method and random numbers. This code is highly applied in designing nuclear reactors, detectors, nuclear well logging, medical radiation, etc. [23-28]. To use the code, an input file has to be prepared with certain sections [29].

The various sections of an input file in the MCNPX code include a cell card, surface card, and data card. The cell card, which is defined based on the geometry of the detector, contains 5 cells in this manuscript. The cells are shown in Figure 2.

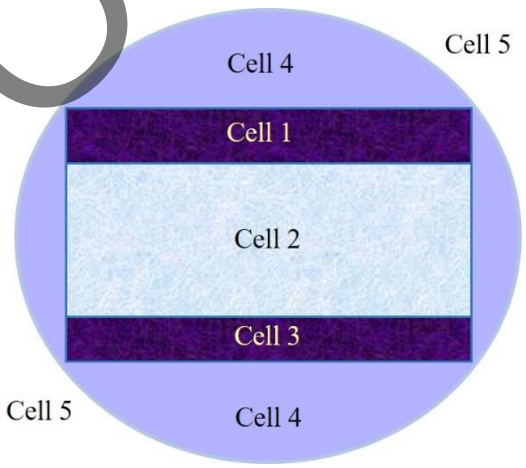

Figure 2. Display of cells defined in MCNPX code

Cell 1 is a steel plate ($10\times10\times Z_1$ cm) which Z_1 has to be optimized. Cell 2 is a volume of air or P10 gas at 1 atmosphere of air pressure with ($10\times10\times0.3$ cm) in dimensions. Cell 3 is a steel plate measuring $10\times10\times0.1$ cm^3. The body of the device is made of Plexiglas with a thickness of 1 cm. Cell 4 is the space inside a sphere, except for the detector, which is where the converter and high-energy X-ray source are located. Cell 5 is the whole space outside the sphere, which does not contain any matter.

A micromesh was added to the set of these cells which is placed between the two upper and lower electrodes, and its exact location is determined by

optimization. Thus, the region between the upper electrode and the micromesh is the drift region, and the region between the micromesh and the lower electrode is the multiplication region. The gases that were used to fill the space of the detector are air and P-10, and the results are obtained for each of these gases separately. Air is a combination of various elements with percentages matching to ICRU report [30, 31]. P10 gas is also a combination of 90% argon and 10% methane. The source used in this research is a high-energy X-ray source with an energy of more than 2 MeV, which is irradiated perpendicularly to the converter. A neutron beam was produced by interaction between high-energy X-ray and converter that this beam crosses to the drift region of the detector. The Electron beam was produced by the interaction of the neutron beam with the gas in the drift region and the converter layer. In MCNPX 2.7e code, different tallies have been used to calculate the number of electrons in the drift and multiplication regions, the number of electrons crossing to the drift region from the upper electrode, the deposited dose in the drift and the multiplication regions, and the deposited dose inside the micromesh holes. Mesh tally type 1 has been applied to calculate the depth-dose in the various regions of the detector. Input file is written to optimize Micromegas detector.

2.3. Calculation of the Detector Current

The number of electrons produced by a high-energy photon (n_0) is equal to the product of the photoneutron production efficiency (γ), the amount of deposited energy by a neutron (E) divided by the energy required to produce an ion pair in the air (W=35 eV) according to Equation 1.

$$n_0 = \gamma E/W \quad (1)$$

The detector current is equal to Equation 2 as follows:

$$I = \frac{kn_0e}{t} = \frac{k\gamma Ee}{tw} \quad (2)$$

Where k is the multiplication factor of the gas (10^5), e is the electron charge, and t is the time of charge collection equal to 0.015 μs.

3. Results

3.1. Calculating the Efficiency of Photoneutron Production by Converter Layer

For calculating the efficiency of photoneutron production, the neutron production per photon versus neutron energy production by impact of 7.6 MeV and 2.3 MeV X-ray energy the tungsten and D_2O converter were calculated that the results were shown in Figure 3a and 3b.

According to Figure 3, the maximum efficiency of photoneutron production for D_2O convertor in 60 keV (neutron energy) and for W converter in 120 keV (neutron energy) are $\gamma=2\times10^{-5}$ and $\gamma=1.5\times10^{-5}$, respectively.

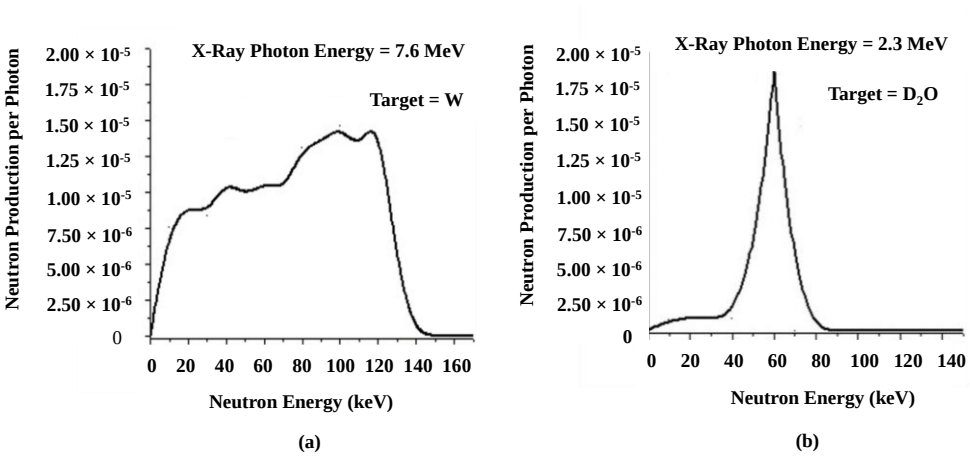

Figure 3. Production of photoneutrons from a target: (a) tungsten (b) heavy water

3.2. Micromegas Optimization for Converting Neutron to Electron

Each of these generated photoneutron spectra can be defined as a neutron source in the MCNPX code and the response of the detector to this neutron spectrum can be obtained. By interaction of neutron spectrum of Figure 3b with steel layer, the number of output electrons from upper electrode to drift region changed with changing the thickness of input window (upper steel layer) that were shown in Figure 4a for air (gas detector) and Figure 4b for P10 (gas detector).

According to MCNPX code results, the optimum thickness of the upper steel electrode for air and P10 gas is 0.0026 cm. According to Figure 5, the whole space of the detector would be divided into 750000 equal cube meshes (0.2×0.2 cm^2) and 0.001 cm in thickness (2500 meshes on the surface of the detector and 300 meshes in the vertical direction).

The diagrams of energy deposited in multiplication and drift regions show as a function of the height of the detector for air and P10 gas in the presence of a micromesh in Figure 6a and 6b.

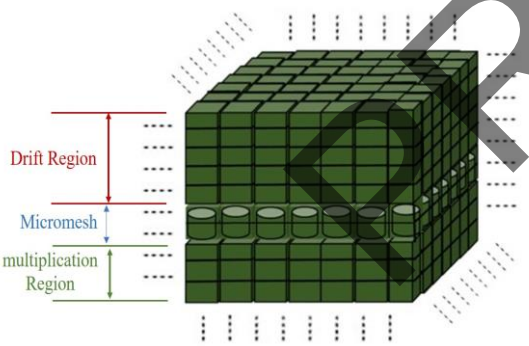

Figure 5. Display meshing of the entire detector space

3.3. Micromegas Response to High-Energy X-Ray

The total dose in air sensitive region of the detector with the volume of 2×10^{-4} cm^3 is equal to 1×10^{9} Gy. As a result, the amount of deposited energy for one neutron (E) would be equal to 5.16×10^{-19} J or 3.22 eV.

By using Equations 1 and 2, the output current of the detector for one photon is equal to 5.12 pA, which is a suitable number for the input of an amplifier that is connected to the Micromegas detector.

4. Discussion

This research aimed to detect high-energy X-rays using a Micromegas detector with photoneutron converter layers. First, the efficiency of photoneutron production by some different converter layers was calculated using Monte Carlo simulation. The threshold energy of these converters for photoneutron production is given in Table 1. The threshold energy data in Table 1 shows that ^{9}Be, ^{2}D, ^{6}Li, ^{13}C, ^{7}Li, and ^{nat}W can detect photons with energy greater than 1.667 MeV, 2.225 MeV, 3.697 MeV, 4.9 MeV, 7.251 MeV, and 7.6 MeV, respectively.

Every converter can be used to detect special X-ray with energy higher than 1.667 MeV. For example, the heavy water and the natural tungsten are proper to detect 2.3 MeV and 7.6 MeV high-energy X-ray, respectively. The probability of neutron production by 2.3 MeV high-energy X-ray with D_2O convertor and 7.6 MeV with natural tungsten converter, were shown in Figure 2a and b. Heavy water shows a sharper neutron energy response compared to tungsten. With

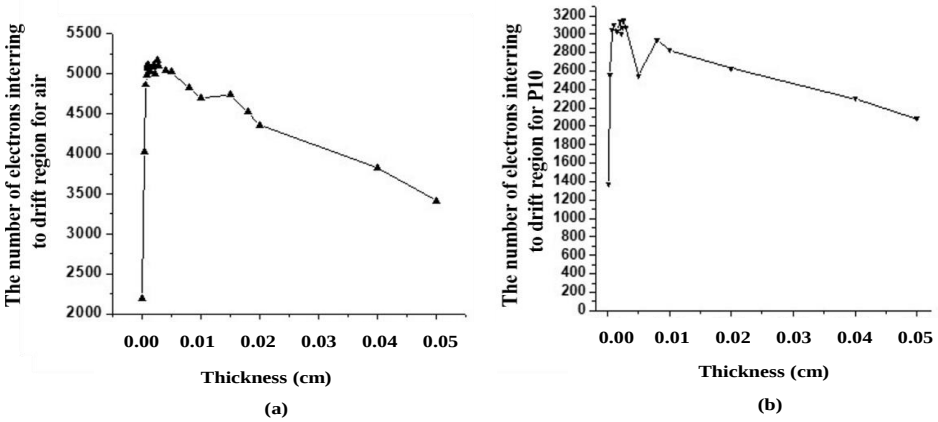

Figure 4. The number of electrons crossing from the upper electrode to the drift region for (a) air (b) P10

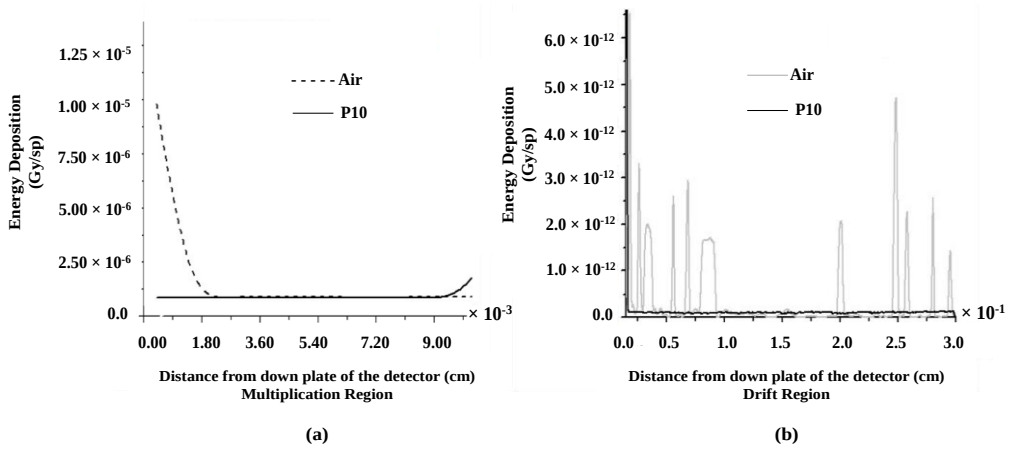

Figure 6. The Energy deposition in the presence of micromesh:(a) in the multiplication region (b) in the drift region

Table 1. Threshold energy of different materials to convert the high-energy X-rays to low-energy neutrons

Target material	^{9}Be	^{2}D	^{6}Li	^{13}C	^{7}Li	^{nat}W
Threshold energy(MeV)	1.667	2.225	3.697	4.9	7.251	7.6

mixing of the elements in Table 1 as a new material, the operator can be detecting the photon with energy larger than 1.667 MeV directly without changing the target.

After the photon is converted to a neutron, the neutron travels to the detector region and after interaction with air or P10 gas, remains the dose in all regions of the detector. As observed in Figure 6, in the drift region and near micromesh in the air, more doses would be remained compared to P10. Almost all over the multiplication region, the energy deposited in the air is bigger compared to P10. Therefore, the air is more suitable than P10 for the detection of neutrons created from photoneutron phenomenon. The dose of neutrons in the sensitive area of the detector causes the ionization of the ideal active gas (air) and the generated electrons multiply due to the strong electric field. The output current of the detector for a photon with an energy of 2.3 MeV, which is equal to 5.12 pA, is large enough to be detected using current amplifier circuits.

5. Conclusion

Using MCNPX code, a Micromegas detector (10×10×0.3 cm) has been optimized to detect 2.3 MeV high-energy X-ray detection. D_2O is the proper convertor to change the high-energy X-ray into a photoneutron that can be detected by Micromegas. In general, the response of the detector has been optimized based on the gas type, and the thickness of the upper electrode. The optimum thickness of the upper electrode is 0.0026 cm for air and P10 gas in the detector. Also, the electron production in air is larger than P10. The results show that this detector has the ability to detect high-energy X-rays with energy above 2 MeV.

References

1- Lu Lu, Mingzi Sun, Qiuyang Lu, Tong Wu, and Bolong Huang, "High energy X-ray radiation sensitive scintillating materials for medical imaging, cancer diagnosis and therapy." *Nano Energy*, Vol. 79p. 105437, (2021).

2- Marcia Dutra R Silva, "Ionizing radiation detectors." *Evolution of Ionizing Radiation Research*, pp. 189-209, (2015).

3- Georges Charpak, R Bouclier, T Bressani, J Favier, and Č Zupančič, "The use of multiwire proportional counters to select and localize charged particles." *Nuclear Instruments and Methods*, Vol. 62 (No. 3), pp. 262-68, (1968).

4- A Oed, "Micro pattern structures for gas detectors." *Nuclear Instruments and Methods in Physics Research Section A: Accelerators, Spectrometers, Detectors and Associated Equipment*, Vol. 471 (No. 1-2), pp. 109-14, (2001).

5- VLADIMIR Peskov, BD Ramsey, and P Fonte, "Surface streamer breakdown mechanisms in microstrip gas counters." *Nuclear Instruments and Methods in Physics Research Section A: Accelerators, Spectrometers, Detectors and Associated Equipment,* Vol. 392 (No. 1-3), pp. 89-93, (1997).

6- Kh U Abraamyan *et al.*, "The MPD detector at the NICA heavy-ion collider at JINR." *Nuclear Instruments and Methods in Physics Research Section A: Accelerators, Spectrometers, Detectors and Associated Equipment,* Vol. 628 (No. 1), pp. 99-102, (2011).

7- Alessandro Caratelli, "Research and development of an intelligent particle tracker detector electronic system." *EPFL*, (2019).

8- JE Bateman *et al.*, "Gas microstrip x-ray detectors for application in synchrotron radiation experiments." *SCAN-9909062*, (1999).

9- Xuan Lian, Hiroyuki Takahashi, Hiroaki Miyoshi, Yuki Mitsuya, and Kenji Shimazoe, "Development of a transparent single-grid-type micro-strip gas chamber based on LCD technology." *Journal of nuclear science and technology*, Vol. 55 (No. 7), pp. 805-11, (2018).

10- FD vd Berg *et al.*, "Study of inclined particle tracks in micro strip gas counters." *Nuclear Instruments and Methods in Physics Research Section A: Accelerators, Spectrometers, Detectors and Associated Equipment,* Vol. 349 (No. 2-3), pp. 438-46, (1994).

11- EF Barasch *et al.*, "A medical imaging microstrip gas counter." in *2000 IEEE Nuclear Science Symposium. Conference Record (Cat. No. 00CH37149)*, (2000), Vol. 3: *IEEE*, pp. 23/22-23/25 vol. 3.

12- Hiroyuki Takahashi *et al.*, "The transparent microstrip gas counter." *Nuclear Instruments and Methods in Physics Research Section A: Accelerators, Spectrometers, Detectors and Associated Equipment,* Vol. 623 (No. 1), pp. 123-25, (2010).

13- Georges Charpak, "Electronic imaging of ionizing radiation with limited avalanches in gases." *Reviews of modern physics*, Vol. 65 (No. 3), p. 591, (1993).

14- Yannis Giomataris, Ph Rebourgeard, Jean Pierre Robert, and Georges Charpak, "MICROMEGAS: a high-granularity position-sensitive gaseous detector for high particle-flux environments." *Nuclear Instruments and Methods in Physics Research Section A: Accelerators, Spectrometers, Detectors and Associated Equipment,* Vol. 376 (No. 1), pp. 29-35, (1996).

15- S Andriamonje *et al.*, "New neutron detectors based on Micromegas technology." *Nuclear Instruments and Methods in Physics Research Section A: Accelerators, Spectrometers, Detectors and Associated Equipment,* Vol. 525 (No. 1-2), pp. 74-78, (2004).

16- J Pancin *et al.*, "Neutron detection in high γ background using a micromegas detector." *Nuclear Instruments and Methods in Physics Research Section A: Accelerators, Spectrometers, Detectors and Associated Equipment,* Vol. 572 (No. 2), pp. 859-65, (2007).

17- J Pancin *et al.*, "Piccolo Micromegas: First in-core measurements in a nuclear reactor." *Nuclear Instruments and Methods in Physics Research Section A: Accelerators, Spectrometers, Detectors and Associated Equipment,* Vol. 592 (No. 1-2), pp. 104-13, (2008).

18- S Khezripour, A Negarestani, and MR Rezaie, "Investigating the response of Micromegas detector to low-energy neutrons using Monte Carlo simulation." *Journal of Instrumentation*, Vol. 12 (No. 08), p. P08007, (2017).

19- A Cools *et al.*, "Neutron and beta imaging with Micromegas detectors with optical readout." *Nuclear Instruments and Methods in Physics Research Section A: Accelerators, Spectrometers, Detectors and Associated Equipment,* Vol. 1048p. 167910, (2023).

20- GK Fanourakis *et al.*, "The use of the Micromegas technology for a new imaging system." *Nuclear Instruments and Methods in Physics Research Section A: Accelerators, Spectrometers, Detectors and Associated Equipment,* Vol. 527 (No. 1-2), pp. 62-67, (2004).

21- Stephan Aune *et al.*, "X-ray detection with Micromegas with background levels below 10− 6keV− 1cm− 2s− 1." *Journal of Instrumentation*, Vol. 8 (No. 12), p. C12042, (2013).

22- F Belloni, F Gunsing, and T Papaevangelou, "Micromegas for neutron detection and imaging." *Modern Physics Letters A*, Vol. 28 (No. 13), p. 1340023, (2013).

23- K Sedlačková, B Zaťko, A Šagátová, M Pavlovič, V Nečas, and M Stacho, "MCNPX Monte Carlo simulations of particle transport in SiC semiconductor detectors of fast neutrons." *Journal of Instrumentation*, Vol. 9 (No. 05), p. C05016, (2014).

24- Kenneth Allen, Travis Knight, and Samuel Bays, "Benchmark of advanced burner test reactor model using MCNPX 2.6. 0 and ERANOS 2.1." *Progress in Nuclear Energy*, Vol. 53 (No. 6), pp. 633-44, (2011).

25- C Guardiola, K Amgarou, F García, C Fleta, D Quirion, and M Lozano, "Geant4 and MCNPX simulations of thermal neutron detection with planar silicon detectors, 2011." ed: JINST.

26- CALICE collaboration and C Adloff, "Validation of GEANT4 Monte Carlo Models with a Highly Granular Scintillator-Steel Hadron Calorimeter, 2013." ed: JINST.

27- Mehdi Hassanpour, Marzieh Hassanpour, Mohammadreza Rezaie, Saeedeh Khezripour, Mohammad Rashed Iqbal Faruque, and Mayeen Uddin Khandaker, "The application of graphene/h-BN metamaterial in medical linear accelerators for reducing neutron leakage in the treatment room." *Physical and Engineering Sciences in Medicine*, Vol. 46 (No. 3), pp. 1023-32, (2023).

28- S Khezripour, N Zarei, and MR Rezaie, "Estimation of granite radiation hazards of Deh Siahan village in Rafsanjan

city." *Journal of Instrumentation*, Vol. 17 (No. 08), p. T08011, (2022).

29- Laurie S Waters *et al.*, "The MCNPX Monte Carlo radiation transport code." in *AIP conference Proceedings*, (2007), Vol. 896 (No. 1): *American Institute of Physics*, pp. 81-90.

30- Joakim Medin, Pedro Andreo, and Stefaan Vynckier, "Comparison of dosimetry recommendations for clinical proton beams." *Physics in Medicine & Biology*, Vol. 45 (No. 11), p. 3195, (2000).

31- Bradley P McCabe, Michael A Speidel, Tina L Pike, and Michael S Van Lysel, "Calibration of GafChromic XR-RV3 radiochromic film for skin dose measurement using standardized x-ray spectra and a commercial flatbed scanner." *Medical physics*, Vol. 38 (No. 4), pp. 1919-30, (2011).